ISSN 0915-633X

NATIONAL INSTITUTE FOR FUSION SCIENCE

Self-organization of Two-dimensional Incompressible Viscous Flow in a Friction-free Box

Y. Kondoh, M. Yoshizawa, A. Nakano and T. Yabe

(Received - Oct. 11, 1995)

NIFS-381 Oct. 1995

RESEARCH REPORT
NIFS Series

NAGOYA, JAPAN

Self-organization of two-dimensional incompressible viscous flow in a friction-free box

Y. Kondoh, M. Yoshizawa, A. Nakano and T. Yabe †

Dept. of Electronic Engineering, Gunma University, Kiryu, Gunma 376, Japan

†*Dept. of Energy Sciences, Tokyo Institute of Technology, Yokohama 226, Japan*

Abstract

The process by which self-organization occurs for two-dimensional incompressible viscous flow in a friction-free box is investigated theoretically with the use of numerical simulations. It is shown by an eigenfunction spectrum analysis that two basic processes for the self-organization are the spectrum transfer by nonlinear couplings and the selective dissipation among the eigenmodes of the dissipative operator, and they yield spectrum accumulation at the lowest eigenmode. It is also clarified that an important process during nonlinear self-organization is an interchange between the dominant operators, which leads to a final self-similar coherent structure, determined uniquely by the lowest eigenmode of the dissipative operator.

PACS numbers: 47.10.+g, 47.25.-c, 52.35.Mw, 52.35.Ra

I. INTRODUCTION

Theories and numerical investigations have been described for self-organization in three-dimensional (3D) magnetohydrodynamic (MHD) plasmas [1–5], two-dimensional (2D) MHD plasmas [6, 7], 2D incompressible viscous fluids [8–12], and solitons described by the Korteweg-de Vries (KdV) equation [13–15]. As Refs. [14, 15] have pointed out, most of these theories on self-organization involve a logic that has in common the following four conceptual elements: (a) the system is described by dissipative nonlinear partial differential equations; (b) in the absence of dissipation, the system has three or more quadratic or higher-order conserved quantities; (c) when dissipation is introduced, one conserved quantity, $A(q)$, decays faster than the others, $B(q)$, where A and B are functionals of the field variables $q(t, \mathbf{x})$, this feature being known as "selective dissipation" between the invariants $A(q)$ and $B(q)$; and (d) the self-organized state is determined by mininizing A under the constraint that B is held constant. Dynamical systems of interest having n variables $q_i(t, \mathbf{x})$, with $i = 1, 2, ...n$, can generally be described by the following equations of motion

$$\frac{\partial q_i}{\partial t} = L_i^N[\mathbf{q}] \; + \; L_i^D[\mathbf{q}] \, , \tag{1}$$

where $L_i^N[\mathbf{q}]$ and $L_i^D[\mathbf{q}]$ denote the nondissipative and dissipative dynamic operators, respectively, which may be either linear or nonlinear [16, 17]. In the conventional theories of self-organization mentioned above, the nondissipative operators $L_i^N[\mathbf{q}]$ are assumed to be dominant throughout the entire self-organization process, with the dissipative operators $L_i^D[\mathbf{q}]$ assumed to be minor and thus capable of being handled perturbatively. Due to this implicit assumption, the self-organized states derived by the conventional theories with the use of the conceptual element (d) have no dependence on the dissipative operators $L_i^D[\mathbf{q}]$ or on the dissipation parameters contained therein [14].

On the other hand, if we start from a definition for the self-organized state as that state for which the rate of change for the autocorrelations of instantaneous values is minimum, then the self-organized state so derived does depend explicitly on the dissipative operator of the dynamical system [16–18]. Some simulations [18, 19] have reported data that show the dependence of the self-organized state on the profile of the dissipation parameters. Theoretical analysis and numerical simulations for the self-organization of MHD plasmas [16–18, 20, 21] and solitons described by the KdV equation with a viscous dissipation term [15] indicate that three basic processes for the self-organization are (1) spectrum transfer and (2) selective dissipation among the eigenmodes of the dissipative operators $L_i^D[\mathbf{q}]$, and (3) interchange between the dominant operators from the nondissipative nonlinear operators $L_i^N[\mathbf{q}]$ to the dissipative operators $L_i^D[\mathbf{q}]$ in the later phase of self-organization. The three basic processes lead to a final self-similar coherent structure of the self-organized state that is determined uniquely by the eigenfunction of the operators $L_i^D[\mathbf{q}]$ with the lowest eigenvalue.

In this paper, we present a theoretical and numerical investigation of the process by which self-organization occurs for a 2D incompressible viscous flow in a friction-free box. We will show that the self-organized state in this flow is the lowest eigenmode of the dissipative operator, resulting from the three basic processes of (1)-(3) mentioned above. In Sec. II, we present a theory of the self-organization and the eigenfunction spectrum analysis [16, 17] applied to the 2D incompressible viscous flow in a friction-free box. Results of a simulation of 2D Navier-Stokes flows and discussion are presented in Sec. III.

II. THEORY OF SELF – ORGANIZATION

We apply here the self-organization theory of [16, 17], which is based on the realization of the coherent sturcture with the minimum change rate of autocorrelations

for their instantaneous values, to 2D incompressible viscous fluids. Taking the curl of the Navier-Stokes equation, we use the following vorticity representation

$$\frac{\partial \omega}{\partial t} = -(\mathbf{u}\cdot\nabla)\omega + \nu\nabla^2\omega, \tag{2}$$

where $\mathbf{u}$ is the fluid velocity, $\omega = \nabla \times \mathbf{u}$ is the vorticity, ν is the kinematic viscosity, and $\nabla \cdot \mathbf{u} = 0$. The nondissipative and dissipative operators $L_t^N[\mathbf{q}]$ and $L_t^D[\mathbf{q}]$ of Eq.(1) correspond, respectively, to the $-(\mathbf{u}\cdot\nabla)\omega$ term and the $\nu\nabla^2\omega$ term in Eq.(2). The global autocorrelation W_ω of ω and its dissipation rate $\partial W_\omega/\partial t$ are written, respectively, as $W_\omega = \int \omega\cdot\omega \, dV$ and $\partial W_\omega/\partial t = -2\int \omega\cdot(\nu\nabla\times\nabla\times\omega)\, dV$, where $\nabla\cdot\omega = 0$ is used. Using the variational calculus to find the self-organized state for which the rate of change for the autocorrelations of instantaneous values is minimum, and defining a functional F with the use of a Lagrange multiplier α as $F \equiv -\partial W_\omega/\partial t - \alpha W_\omega$, we obtain the following Euler-Lagrange equation from $\delta F = 0$ for the self-organized state ω^* [16, 17]:

$$\nabla \times \nabla \times \omega^* = \frac{\alpha}{2\nu}\omega^* . \tag{3}$$

When we work in the velocity representation of the Navier-Stokes equation, we obtain the same type of Euler-Lagrange equation for the velocity $\mathbf{u}^*$ at the self-organized state, as follows [16, 17]:

$$\nabla \times \nabla \times \mathbf{u}^* = \frac{\alpha}{2\nu}\mathbf{u}^* . \tag{4}$$

The eigenfunctions of Eqs.(3) and (4) can be obtained for given boundary values of $\mathbf{u}$ and ω, as boundary value problems. Using the same procedure in [16, 17], we obtain the following:

$$W_\omega^* = e^{-\alpha t} W_{\omega R}{}^* = e^{-\alpha t}\int [\omega_R{}^*(\mathbf{x})]^2 \, dV \tag{5}$$

$$\omega^* = \omega_R{}^*(\mathbf{x})\, e^{-\frac{\alpha}{2}t} , \tag{6}$$

$$W_{\mathbf{u}}^{*} \;=\; \mathrm{e}^{-\alpha t} W_{\mathbf{u}R^{*}} \;=\; \mathrm{e}^{-\alpha t} \int [\mathbf{u}_{R}{}^{*}(\mathbf{x})]^{2}\, \mathrm{d}V \tag{7}$$

$$\mathbf{u}^{*} \;=\; \mathbf{u}_{R}{}^{*}(\mathbf{x})\, \mathrm{e}^{-\frac{\alpha}{2} t}\,, \tag{8}$$

where $\omega_{R}{}^{*}(\mathbf{x})$ and $\mathbf{u}_{R}{}^{*}(\mathbf{x})$ denote the eigensolutions for Eqs.(3) and (4) for given boundary values, which are supposed to be realized at the state with the minimum dissipation rate. We find from Eqs.(5) - (8) that the eigenfunctions of $\omega^{*}(\mathbf{x})$ and $\mathbf{u}^{*}(\mathbf{x})$ for the dissipative operator $-\nu\nabla\times\nabla\times\omega$ (or $-\nu\nabla\times\nabla\times\mathbf{u}$) constitute the self-organized and self-similar decay phase during the time evolution of the present dynamical system.

From $\delta^{2}F \geq 0$, we obtain the following associated eigenvalue problems for critical perturbations $\delta\omega$ and $\delta\mathbf{u}$ that make $\delta^{2}F$ vanish, and the condition for the state with the minimum dissipation rate [16, 17]:

$$\nabla\times\nabla\times\delta\omega_{k} \;-\; \lambda_{k}^{2}\,\delta\omega_{k} \;=\; 0\,, \tag{9}$$

$$\nabla\times\nabla\times\delta\mathbf{u}_{k} \;-\; \lambda_{k}^{2}\,\delta\mathbf{u}_{k} \;=\; 0\,, \tag{10}$$

$$0 \;<\; \alpha \;\leq\; \alpha_{1}\,. \tag{11}$$

Here, $\lambda_{k}^{2} \equiv \alpha_{k}/2\nu$, α_{k} and λ_{k} are the eigenvalues, $\delta\omega_{k}$ and $\delta\mathbf{u}_{k}$ denote the eigensolutions, α_{1} is the smallest positive eigenvalue, the boundary conditions are $\delta\omega_{\mathrm{w}}\cdot\mathrm{d}\mathbf{S} = 0$, and the subscript w denotes the value at the boundary wall. When we work inside a square friction-free box in the x, y plane, with edge length 1, Eq.(3) becomes equivalent to Eq.(9). Therefore, the decay constant α of the autocorrelation W_{ω}^{*} (or $W_{\mathbf{u}}^{*}$) at the self-organized state in Eq.(5) [or Eq.(7)] is equal to the smallest eigenvalue α_{1} ($= 2\nu\lambda_{1}^{2}$), and ω^{*} coinsides with the lowest eigensolution $\delta\omega_{1}$.

We now describe a physical picture for the self-organization process by using an eigenfunction spectrum analysis associated with the dissipative operator [16, 17]. Owing to the the self-adjoint property of the present dissipative operator [16, 17], the eigenfunctions, $\mathbf{a}_k$, for the associated eigenvalue problem of Eq.(9) form a complete orthogonal set and the appropriate normalization is written as:

$$\begin{aligned} \int \mathbf{a}_k \cdot (\nabla \times \nabla \times \mathbf{a}_j)\, \mathrm{d}V &= \int \mathbf{a}_j \cdot (\nabla \times \nabla \times \mathbf{a}_k)\, \mathrm{d}V \\ &= \lambda_k^2 \int \mathbf{a}_j \cdot \mathbf{a}_k\, \mathrm{d}V \\ &= \lambda_k^2\, \delta_{jk}\ , \end{aligned} \tag{12}$$

where $\nabla \times \nabla \times \mathbf{a}_k - \lambda_k^2\, \mathbf{a}_k = 0$ is used. For the present case inside a square friction-free box with edge length 1 in the x, y plane, the normalized orthogonal eigensolutions of $\mathbf{a}_{\omega k}$ for the vorticity and $\mathbf{a}_{uk}$ for the velocity are obtained as follows:

$$\mathbf{a}_{\omega k} = 2 \sin l_k \pi x \sin m_k \pi y\, \mathbf{k}, \tag{13}$$

$$\mathbf{a}_{uk} = \frac{2}{\sqrt{l_k^2 + m_k^2}} \left(m_k \sin l_k \pi x \cos m_k \pi y\, \mathbf{i} - l_k \cos l_k \pi x \sin m_k \pi y\, \mathbf{j} \right), \tag{14}$$

where $\lambda_k^2 = \pi^2 (l_k^2 + m_k^2)$, $l_k \geq 1$, $m_k \geq 1$, l_k and m_k are mode numbers in x and y directions, respectively, and $\mathbf{i}$, $\mathbf{j}$ and $\mathbf{k}$ are the unit vectors in x, y, and z directions, respectively. Here, $\nabla \times \mathbf{a}_{uk} = \pi \sqrt{l_k^2 + m_k^2}\, \mathbf{a}_{\omega k}$. The distributions of ω and $\mathbf{u}$ at each instant can then be expanded with the use of these normalized orthogonal eigenfunctions $\mathbf{a}_{\omega k}$ and $\mathbf{a}_{uk}$, as follows:

$$\omega = \sum_{k=1}^{\infty} c_{\omega k}\, \mathbf{a}_{\omega k}\ . \tag{15}$$

$$\mathbf{u} = \sum_{k=1}^{\infty} c_{uk}\, \mathbf{a}_{uk}\ , \tag{16}$$

where $\pi \sqrt{l_k^2 + m_k^2}\, c_{uk} = c_{\omega k}$, and the spectra of $c_{\omega k}$ and c_{uk} ($k = 1, 2, \cdots$) depend now on time t. Substituting Eqs.(15), (16) and (9) into Eq.(2), we obtain the following:

$$\sum_{k=1}^{\infty} \frac{\partial c_{\omega k}}{\partial t} \mathbf{a}_{\omega k} = (\sum_{k=1}^{\infty} c_{uk}\, \mathbf{a}_{uk} \cdot \nabla)(\sum_{k=1}^{\infty} c_{\omega k}\, \mathbf{a}_{\omega k}) - \sum_{k=1}^{\infty} \nu \lambda_k^2\, c_{\omega k} \mathbf{a}_{\omega k} \,. \qquad (17)$$

With the use of Eqs.(13) and (14), the nonlinear coupling terms and the dissipative terms in Eq.(17) are written respectively as follows:

$$\begin{aligned}
&\sum_{i=1}^{\infty}\sum_{j=1}^{\infty} (\, c_{ui}\, \mathbf{a}_{ui} \cdot \nabla\,) c_{\omega j}\, \mathbf{a}_{\omega j} \\
&= \sum_{i=1}^{\infty}\sum_{j=1}^{\infty} \frac{c_{\omega i}\, c_{\omega j}}{l_i^2 + m_i^2} \{\, (m_i l_j - l_i m_j)[\, \sin\,(l_i + l_j)\pi x \, \sin\,(m_i + m_j)\pi y \\
&\qquad\qquad - \sin\,(l_i - l_j)\pi x \, \sin\,(m_i - m_j)\pi y\,] \\
&\qquad - (m_i l_j + l_i m_j)[\, \sin\,(l_i + l_j)\pi x \, \sin\,(m_i - m_j)\pi y \\
&\qquad\qquad - \sin\,(l_i - l_j)\pi x \, \sin\,(m_i + m_j)\pi y\,]\,\}\, \mathbf{k} \,. \qquad (18)
\end{aligned}$$

$$-\sum_{k=1}^{\infty} \nu \lambda_k^2\, c_{\omega k} \mathbf{a}_{\omega k} = -\sum_{k=1}^{\infty} 2\nu\pi^2 (l_k^2 + m_k^2)\, c_{\omega k} \sin\, l_k \pi x \, \sin\, m_k \pi y \, \mathbf{k} \,. \qquad (19)$$

We see the followings from Eq.(18): When $i = j$, the nonlinear coupling terms are equal to zero, i.e. the eigenmode (l_i, m_i) does not have the nonlinear coupling with itself. When $i \neq j$, then the nonlinear coupling terms induce spectrum transfers to both the higher and the lower eigenmodes of ($l_i \pm l_j$, $m_i \pm m_j$). The dissipative terms of Eq.(19) show the selective dissipation among the eigenmodes, i.e. the higher spectral components dissipate more rapidly in proportion to the decay constant of $\nu\pi^2(l_k^2 + m_k^2)$. Compareing the right hand sides of Eqs.(18) and (19), we find that after a long term dissipation with the spectrum transfers and the selective dissipation, spectral components $c_{\omega k}$ will become smaller so that $\mid c_{\omega i} c_{\omega j}(m_i l_j \pm l_i m_j)/(l_i^2 + m_i^2) \mid$ $< 2\nu\pi^2(l_k^2 + m_k^2) c_{\omega k}$ even to the lowest eigenmode (1,1), and the dominant operator changes consequently from the nonlinear coupling terms to the dissipative terms.

As reported in [16, 17, 15, 18, 20, 21], we find the following physical picture for the self-organization process from the eigenfunction spectrum analysis shown above with the use of Eqs.(17) - (19): (1) The nondissipative nonlinear operator induces

the spectrum transfer toward both the higher and the lower eigenmode regions of the dissipative operator. (Since there exists a limit to the lower eigenmode, the spectrum transfer toward the lower eigenmode region may yield spectrum accumulation at the lowest eigenmode. On the other hand, there is no limit to the higher eigenmode, the spectrum transfer to the higher eigenmode region may result in the spread of the spectrum to the infinity.) (2) At the same time, the dissipative operator yields the selective dissipation among the eigenmodes of the dissipative operator, i.e. the higher spectral components dissipate more rapidly with decay constants of $\nu\lambda_k^2$. (3) In the later phase of self-organization, there occurs an interchange between the dominant operators from the nondissipative nonlinear operator to the dissipative operator, and the lowest eigenmode persists to the end as a final self-similar coherent structure.

III. COMPUTATIONAL RESULTS AND DISCUSSION

We solve Eq.(2) in dimensionless unit, inside a square friction-free box in the x, y plane, with edge length 1. The fluid velocity $\mathbf{u} = \nabla\psi \times \mathbf{k}$, where the stream function $\psi = \psi(x, y, t)$ is independent of z, as are all other field variables. The vorticity $\omega = \nabla \times \mathbf{u} = \omega\mathbf{k}$, and the relation between ω and ψ is given by

$$\nabla^2\psi \ = \ -\omega \tag{20}$$

We solve the hyperbolic equation of Eq.(2) by using one of two new type schemes, named the CIP (Cubic Interpolated Pseudo-particle) scheme [22, 23] and the KOND (Kernel Optimum Nearly-analytical Discretization algorithm) scheme [24, 25], both of which have high numerical accuracy and stabitilty. We use the SOR (Successive Over-Relaxation) scheme [26] to solve the elliptic type equation of Eq.(20). Numerical procedures at each time step are as follows; 1) solve Eq.(20) by the SOR scheme to get new values of ψ, 2) get new values of $\mathbf{u}$ from the new ψ, 3) solve Eq.(2) by the

CIP scheme or by the KOND scheme to get new values of ω, and 4) go to 1) for the next time step. The boundary conditions at the friction-free wall are given by $\psi_w = 0$ and $\omega_w = 0$, where the subscript w denotes the values at the boundary wall. The simulation domain is implemented on a (101×101) point grid. The time step is $\Delta t = 0.0001$. The kinematic viscosity ν can, in the dimensionless units, be interpreted as the reciprocal of a Reynolds number R based on unit length and a unit initial rms velocity, i.e. $R = \nu^{-1}$.

We show here typical results of simulations for two cases with $R = 500$, whose initial flow structures are different with each other and do not contain the lowest eigenmode $(1,1)$. In these cases, since the smallest eigenvalue corresponding to the eigenmode of $(1,1)$ is $\lambda_1 = \sqrt{2}\,\pi$, the theoretical decay constant α_1 ($= 2\nu\lambda_1^2$) of the autocorrelation $W_{\mathbf{u}}^*$ at the self-organized state in Eq.(7) has the same value of 0.7896×10^{-1}, which was compared with the simulation results.

First, we present typical results of simulations with the use of the CIP scheme for the procedure of 3) to solve Eq.(2). Figure 1 shows the typical time evolution of the vorticity structure during the self-organization process, which starts from an initial flow given by superposition of two eigenmodes of $(1,3)$ and $(2,4)$ with the use of Eq.(14) for the velocity. Here, the bold and the thin lines in the figures show contour plots of positive vorticity and those of negative one, respectively, and the hight of contours is normalized by the maximum absolute value of either the positive or the negative vorticity in each figure. It is seen from the vorticity contours at $t = 0.5$ that the nonlinear process changes the initial simple structure of vorticity at $t = 0$ into the more complicated structure with small scale deformations. The small scale deformations of vorticity structure gradually vanish away, as is seen from the vorticity contours at $t = 0.5$ and $t = 1.5$. The two negative vorticity centers at $t = 1.5$ merge into the larger structure with one negative center at $t = 4$, in the similar way as

reported in [8–12]. Rotating counterclockwise around the center of the box (cf. the vorticity contours at $t = 0.5$, 1.5, 4 and 8 in Fig.1), the two outside positive vorticity centers gradually vanish, as is recognized from the two contour plots of vorticity at $t = 4$ and $t = 8$. We find finally that the simplest structure with one negative vorticity center persists to the end, as is shown in the figure of the contour plots at $t = 32$.

In order to check the physical picture for the self-organization process described in the previous section, we applied the eigenfunction spectrum analysis associated with the dissipative operator [16, 17] to the simulation results of the self-organization process shown in Fig. 1. Multiplying the simulation data of vorticity at each time by the normalized orthogonal eigensolutions $\mathbf{a}_{\omega k}$ of Eq.(13) and integrating the results over the square box, we obtain numerically the spectral components of $c_{\omega k}$ at each time. Figure 2 shows the time evolution of the resultant spectral componets of vorticity during the self-organization process of the flow structure, which are obtained from the simulation data shown in Fig. 1. Here, the horizontal scale represents the square of the spectral eigenvalues $\lambda_k^2 = \pi^2(l_k^2 + m_k^2)$ for eigenmodes (l_k, m_k), and the vertical scale is normalized by the maximum absolute value of either the positive or the negative spectral components $c_{\omega k}$ in each figure. The vorticity spectrum at $t = 0$ is shown to have only two spectral components of $(1, 3)$ and $(2, 4)$, which correspond to the initial flow given by superposition of two eigenmodes of $(1, 3)$ and $(2, 4)$ with the use of Eq.(14) for the velocity. We note here that the vorticity spectral component of eigenmode $(2, 4)$ is larger than that of eigenmode $(1, 3)$ because of the relation $\nabla \times \mathbf{a}_{uk} = \pi\sqrt{l_k^2 + m_k^2}\, \mathbf{a}_{\omega k}$. We find from the spectrum at $t = 0.5$ that the nonlinear process yields the spectrum transfer toward both the higher and the lower spectral eigenmodes, in other words, it yields both fo the normal and the inverse cascades [cf. the vorticity contours at $t = 0.5$ in Fig. 1 and also Eq.(18)]. It is seen from comparisons between two spectra at $t = 0.5$ and $t = 1.5$ that the higher spectral

components dissipate more rapidly. We recognize from the time evolution of spectra after $t = 1.5$ that the spectrum transfer toward the lower eigenmode region yields gradually spectrum accumulation at the lowest eigenmode of $(1,1)$. In the later phase of self-organization, the dominant operator changes from nonlinear coupling terms of Eq.(18) to the dissipative terms of Eq.(19), so that the lowest eigenmode of $(1,1)$ persists to the end, as is shown by the spectrum at $t = 32$. It should be noted here that the eigenmode of $(1,1)$ was not contained in the initial flow at $t = 0$, but has been induced nonlinearly during the self-organization process.

Figure 3 shows the time dependence of the flow energy E for the case of Fig. 1, where E is defined here by $E = \int \mathbf{u} \cdot \mathbf{u}\, dV$ and is equal to the global autocorrelation $W_{\mathbf{u}}$ with respect to the velocity $\mathbf{u}$ [cf. Eq.(7)]. After a rapid decay lasting until around $t \sim 12$, the decay rate of E is seen to become almost constant. At around $t = 25$, the decay constant has a value of 0.790×10^{-1}, which agrees very well with the theoretical decay constant of $\alpha_1 = 2\nu\lambda_1^2 = 0.7896 \times 10^{-1}$.

Next, we present typical results of simulations for another case of different initial flow structure, with the use of the KOND scheme for the procedure of 3) to solve Eq.(2). Figure 4 shows the typical time evolution of the vorticity structure during the self-organization process, which starts from another initial flow given by superposition of two eigenmodes of $(2,4)$ and $(1,5)$ with the use of Eq.(14) for the velocity. It is seen from the vorticity contours at $t = 1$ in Fig. 4 that the nonlinear process changes the initial simple structure of vorticity at $t = 0$ into the more complicated structure with small scale deformations, similarly to the case of Fig. 1. The small scale deformations of vorticity structure gradually vanish away, as is seen again from the vorticity contours at $t = 1$ and $t = 1.5$. Rotating clockwise around the center of the box this time (cf. the vorticity contours at $t = 1$, 1.5, 4 and 10 in Fig.4), the two large positive vorticity centers at $t = 1.5$ merge gradually into the larger structure

with one positive center at $t = 10$. The two outside negative vorticity centers rotate clockwise around the positive vorticity center and gradually vanish again, similarly to the case of Fig. 1. We find finally again that the simplest structure with one positive vorticity center persists to the end, as is shown in the figure of the contour plots at $t = 34$, eventhough the initial flow structure is different from that of the former case shown in Fig. 1.

Figure 5 shows the time evolution of the spectral componets of vorticity during the self-organization process of the flow structure, which are obtained from the simulation data shown in Fig. 4. The vorticity spectrum at $t = 0$ is shown to have only two spectral components of $(2,4)$ and $(1,5)$, which correspond to the initial flow given by superposition of two eigenmodes of $(2,4)$ and $(1,5)$ with the use of Eq.(14) for the velocity. We find again from the spectrum at $t = 1$ that the nonlinear process yields the spectrum transfer toward both the higher and the lower spectral eigenmodes , i.e. both of the normal and the inverse cascades [cf. the vorticity contours at $t = 1$ in Fig. 4 and also Eq.(18)]. It is seen from comparisons between two spectra at $t = 1$ and $t = 1.5$ that the higher spectral components dissipate more rapidly. We recognize again from the time evolution of spectra after $t = 1.5$ that the spectrum transfer toward the lower eigenmode region yields gradually the spectrum accumulation at the lowest eigenmode of $(1,1)$. In the later phase of self-organization, the dominant operator changes from nonlinear coupling terms of Eq.(18) to the dissipative terms of Eq.(19), so that the lowest eigenmode of $(1,1)$ persists to the end, as is shown by the spectrum at $t = 34$. It should be noted here again that the eigenmode of $(1,1)$ was not contained in the initial flow at $t = 0$, but has been induced nonlinearly during the self-organization process, in the same way as the former case of different initial flow structure shown in Fig. 2.

Figure 6 shows the time dependence of the flow energy E for the case of Fig.

4. After a rapid decay lasting until around $t \sim 12$, the decay rate of E is seen to become almost constant again. At around $t = 25$, the decay constant has a value of 0.791×10^{-1}, which agrees very well again with the theoretical decay constant of $\alpha_1 = 2\nu\lambda_1^2 = 0.7896 \times 10^{-1}$.

IV. SUMMARY

We have presented the application of the self-organization theory by one of the authors (Y.K.) [16, 17] to the 2D incompressible viscous fluids in Sec. II. We have shown that the self-organized state predicted by the theory for the vorticity structure inside the square friction-free box is the lowest eigensolution of Eq.(9) and the theoretical decay constant α of the autocorrelation W_ω^* (or $W_{\mathbf{u}}^*$) at the self-organized state in Eq.(5) [or Eq.(7)] is equal to the smallest eigenvalue α_1 ($= 2\nu\lambda_1^2$). We have also described a physical picture for the self-organization process [from Eq.(12) to Eq.(19)], by using the eigenfunction spectrum analysis associated with the dissipative operator [16, 17]. We have clarified following three points from Eqs.(18) and (19): (A) The nonlinear coupling terms induce the spectrum transfers to both the higher and the lower eigenmodes of ($l_i \pm l_j$, $m_i \pm m_j$), while the eigenmode (l_i, m_i) does not have the nonlinear coupling with itself. (B) The dissipative terms yield the selective dissipation among the eigenmodes, i.e. the higher spectral components dissipate more rapidly in proportion to the decay constant of $\nu\pi^2(l_k^2 + m_k^2)$. (C) After a long term dissipation with the spectrum transfers and the selective dissipation, spectral components $c_{\omega k}$ will become smaller so that $| c_{\omega i}c_{\omega j}(m_i l_j \pm l_i m_j)/(l_i^2 + m_i^2) | < 2\nu\pi^2(l_k^2 + m_k^2)c_{\omega k}$ even to the lowest eigenmode $(1, 1)$, and the dominant operator changes consequently from the nonlinear coupling terms to the dissipative terms.

In order to demonstrate the self-organization process predicted by the theory in Sec. II, we have presented in Sec. III the typical results of numerical simulations

for the two different initial flow cases with $R = 500$, whose initial flow structures are simple but do not contain the lowest eigenmode $(1, 1)$. It has been shown by the time evolution of the vorticity contours that the nonlinear process changes at first the initial simple structure into the more complicated structure with small scale deformations. Without dependence on the different initial structures, however, the nonlinear process leads finally to the simplest structure with one vorticity center (cf. Figs. 1 and 4), accompanying the merger of two same sign vorticity centers into the larger structure with one center, in the similar way as reported in [8–12]. It has been shown clearly by the numerical eigenfunction spectrum analysis for the two cases that the nonlinear process yields the spectrum transfer toward both the higher and the lower spectral eigenmodes (i.e. both of the normal and the inverse cascades), and the higher spectral components dissipate more rapidly (i.e. the selective dissipation among the eigenmodes of the dissipative operator). The spectrum transfer toward the lower eigenmode region yields gradually the spectrum accumulation at the lowest eigenmode of $(1, 1)$, which persists to the end, without dependence on the different initial structures (cf. Figs. 2 and 5). It has been shown by the time dependence of the flow energy E obtained numerically for the two cases that, after the initial rapid decay, the decay rate of flow energy E becomes almost constant with a value of 0.790×10^{-1} in Fig. 3 and with that of 0.791×10^{-1} in Fig. 6. Both of the two numerical decay constants agree very well with the theoretical decay constant of $\alpha_1 = 2\nu\lambda_1^2 = 0.7896 \times 10^{-1}$.

The analytical and the numerical investigations for the self-organization of the 2D incompressible viscous flow presented here may lead to the following physical picture for the self-organization process:

(1) The nondissipative nonlinear operator induces the spectrum transfer toward both the higher and the lower eigenmode regions of the dissipative operator. (The

spectrum transfer toward the lower eigenmode region yields spectrum accumulation at the lowest eigenmode. The spectrum transfer to the higher eigenmode region results in the spread of the spectrum to the infinity.)

(2) At the same time, the dissipative operator yields the selective dissipation among the eigenmodes of the dissipative operator, i.e. the higher spectral components dissipate more rapidly with decay constants of $\nu\lambda_k^2$.

(3) In the later phase of self-organization, there occurs an interchange between the dominant operators from the nondissipative nonlinear operator to the dissipative operator, and the lowest eigenmode persists to the end as a final self-similar coherent structure.

The study of the self-organization presented here suggests that the principle of the minimum dissipation rate of enstrophy ($W_\omega = \int \omega \cdot \omega \, dV$) can be used for the theory of self-organization as well as the principle of the minimum dissipation rate of energy ($E = \int \mathbf{u} \cdot \mathbf{u} \, dV$). However, the more essential physics contained fundamentally is the principle of the minimum dissipation rate of autocorrelations ($W_{ii} = \int q_i \cdot q_i \, dV$) in the dynamical systems [17].

It is interesting to note that the physical picture shown above is also common to the two self-organization processes in solitons described by the KdV equation with a viscous dissipation term [15] and in 3D resistive MHD plasmas [21], while this picture has not been applied yet to other nonlinear dissipative dynamical systems.

ACKNOWLEDGMENTS

The authors would like to thank Messrs. N. Kondo, M. Yamaguchi, and T. Fukasawa for their valuable discussion and help on programming for our spectrum analysis. They greatly appreciate valuable discussion and comments on this work by

Professor T. Sato at the National Institute for Fusion Science, Nagoya, Japan, and Dr. J. W. Van Dam at the Institute for Fusion Studies, University of Texas at Austin, U.S.A.. This work was carried out under the collaborative research program at the NIFS, Nagoya, Japan. This work has been supported by a Grant-in Aid for Scientific Research from the Ministry of Education, Science and Culture, Japan. This work was carried out partly under the sponsorship of the U.S.-Japan Joint Institute for Fusion Theory exchange program during the stay of the first author (Y.K.) at the IFS, University of Texas at Austin.

REFERENCES

[1] J. B. Taylor: Phys. Rev. Lett. **33** (1974) 1139.

[2] J. B. Taylor: Rev. Mod. Phys. **58** (1986) 741.

[3] R. Horiuchi and T. Sato: Phys. Rev. Lett. **55** (1985) 211.

[4] R. Horiuchi and T. Sato: Phys. Fluids **29** (1986) 4174.

[5] R. Horiuchi and T. Sato: Phys. Fluids **31** (1988) 1142.

[6] D. Fyfe and D. Montgomery: J. Plasma Phys. **16** (1976) 181.

[7] W. H. Matthaeus and D. Montgomery: Ann. NY Acad. Sci. **357** (1980) 203.

[8] R. H. Kraichnan and D. Montgomery: Rep. Prog. Phys. **43** (1980) 35.

[9] M. Hossain, W. H. Matthaeus and D. Montgomery: J. Plasma Phys. **30** (1983) 479.

[10] W. H. Matthaeus, W. T. Stribling, D. Martinez, S. Oughton and D. Montgomery: Physica D **51** (1991) 531.

[11] W. H. Matthaeus, W. T. Stribling, D. Martinez, S. Oughton and D. Montgomery: Phys. Rev. Lett. **66** (1991) 2731.

[12] D. Montgomery, W. H. Matthaeus, W. T. Stribling, D. Martinez, and S. Oughton: Phys. Fluids A **4** (1992) 3.

[13] A. Hasegawa, Y. Kodama and K. Watanabe: Phys. Rev. Lett. **47** (1981) 1525.

[14] A. Hasegawa: Adv. Phys. **34** (1985) 1.

[15] Y. Kondoh and J. W. Van Dam: Phys. Rev. E **52** (1995) 1721.

[16] Y. Kondoh: Phys. Rev. E **48** (1993) 2975.

[17] Y. Kondoh: Phys. Rev. E **49** (1994) 5546.

[18] Y. Kondoh, Y. Hosaka, J. Liang, R. Horiuchi and T. Sato: J. Phys. Soc. Jpn. **63** (1994) 546.

[19] Y. Ono and M. Katsurai: Nucl. Fusion **31** (1991) 233.

[20] Y. Kondoh, T. Yumoto, M. Yamaguchi, N. Kondo, R. Horiuchi and T. Sato: J. Plasma and Fusion Res. **71** (1995) 432.

[21] N. Kondo and Y. Kondoh: J. Plasma and Fusion Res. **71** (1995) 890.

[22] T. Yabe and E. Takei: J. Phys. Soc. Jpn. **57** (1988) 2598.

[23] T. Yabe and T. Aoki: Comput. Phys. Commun. **66** (1991) 219.

[24] Y. Kondoh: J. Phys. Soc. Jpn. **60** (1991) 2851.

[25] Y. Kondoh, Y. Hosaka and K. Ishii: Computers Math. Applic. **27** (1994) 59.

[26] D. Young: Trans. Amer. Math. Soc. **76** (1954) 92.

Figure captions

Fig.1. Typical time evolution of vorticity structures during self-organization. The initial flow at $t = 0$ is given by superposition of two eigenmodes of $(1, 3)$ and $(2, 4)$ with the use of Eq.(14) for the velocity. The bold and the thin lines show contour plots of positive vorticity and those of negative one, respectively. The hight of contours is normalized by the maximum absolute value of either the positive or the negative vorticity in each figure.

Fig.2. Time evolution of spectral componets of vorticity during self-organization, obtained from the simulation data shown in Fig. 1. Horizontal scale is given by the square of spectral eigenvalues $\lambda_k^2 = \pi^2(l_k^2 + m_k^2)$ for eigenmodes (l_k, m_k). Vertical scale is normalized by the maximum absolute value of either the positive or the negative spectral components $c_{\omega k}$ in each figure.

Fig.3. Time dependence of the flow energy E, defined by $E = \int \mathbf{u} \cdot \mathbf{u} \, dV$, for the case of Fig. 1. The numerical value of the decay constant at around $t = 25$ is 0.790×10^{-1}.

Fig.4. Typical time evolution of vorticity structures during self-organization, where the initial flow at $t = 0$ is given by superposition of two eigenmodes of $(2, 4)$ and $(1, 5)$. The bold and the thin lines show contour plots of positive vorticity and those of negative one, respectively. The hight of contours is normalized by the maximum absolute value of either the positive or the negative vorticity in each figure.

Fig.5. Time evolution of spectral componets of vorticity during self-organization,

obtained from the simulation data shown in Fig. 4. Vertical scale is normalized by the maximum absolute value of either the positive or the negative spectral components $c_{\omega k}$ in each figure.

Fig.6. Time dependence of the flow energy E for the case of Fig. 4. The numerical value of the decay constant at around $t = 25$ is 0.791×10^{-1}.

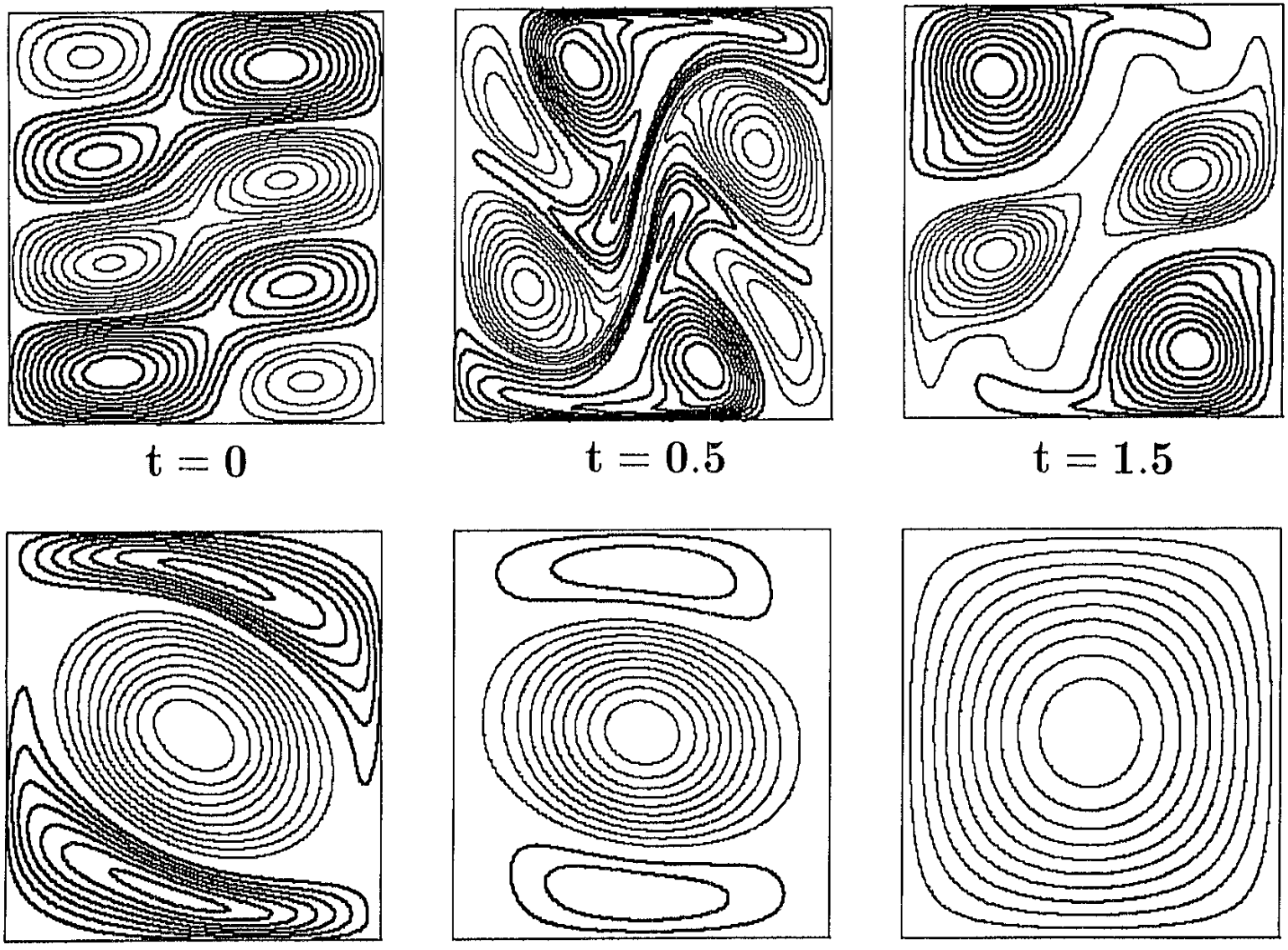

Fig.1

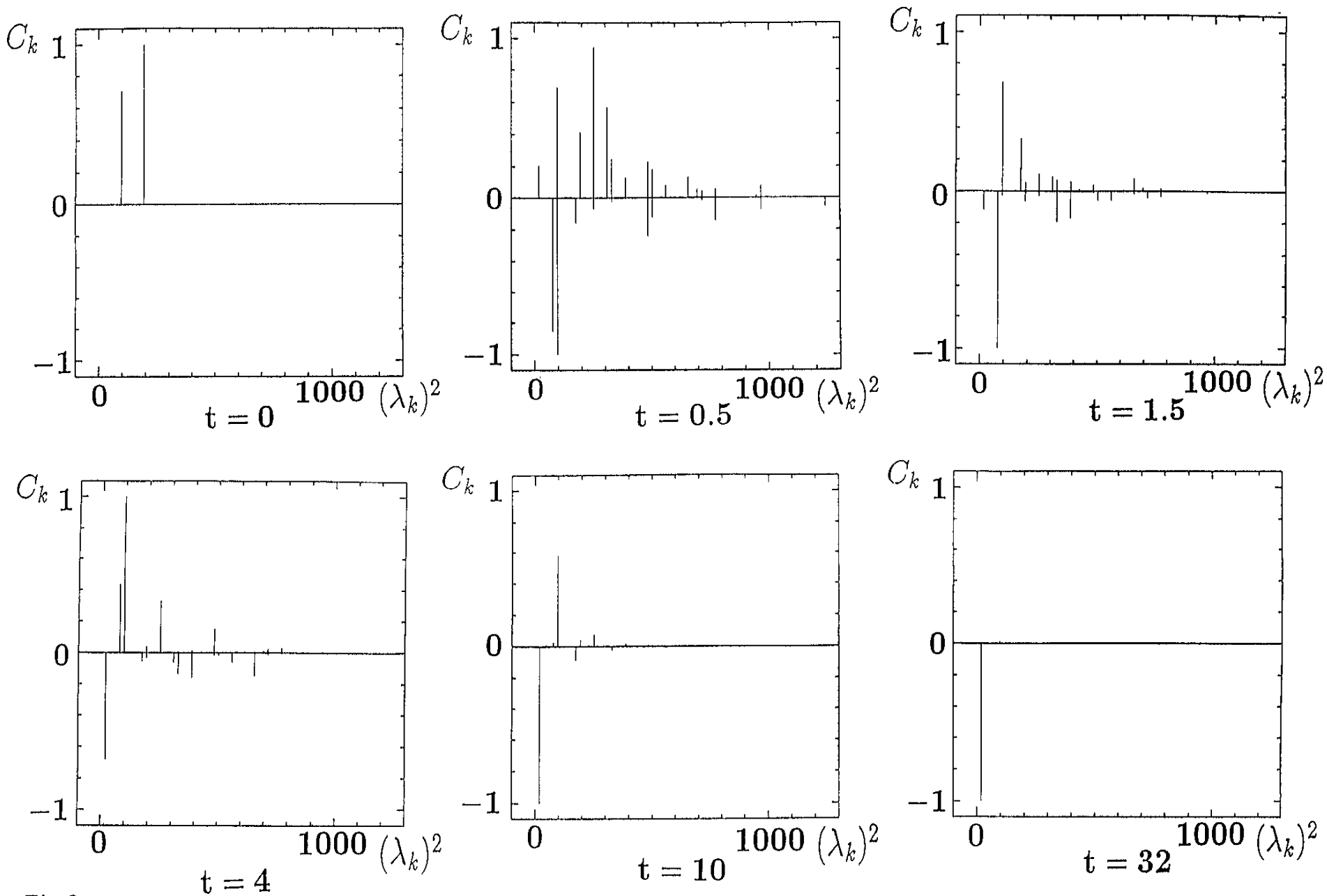

Fig.2

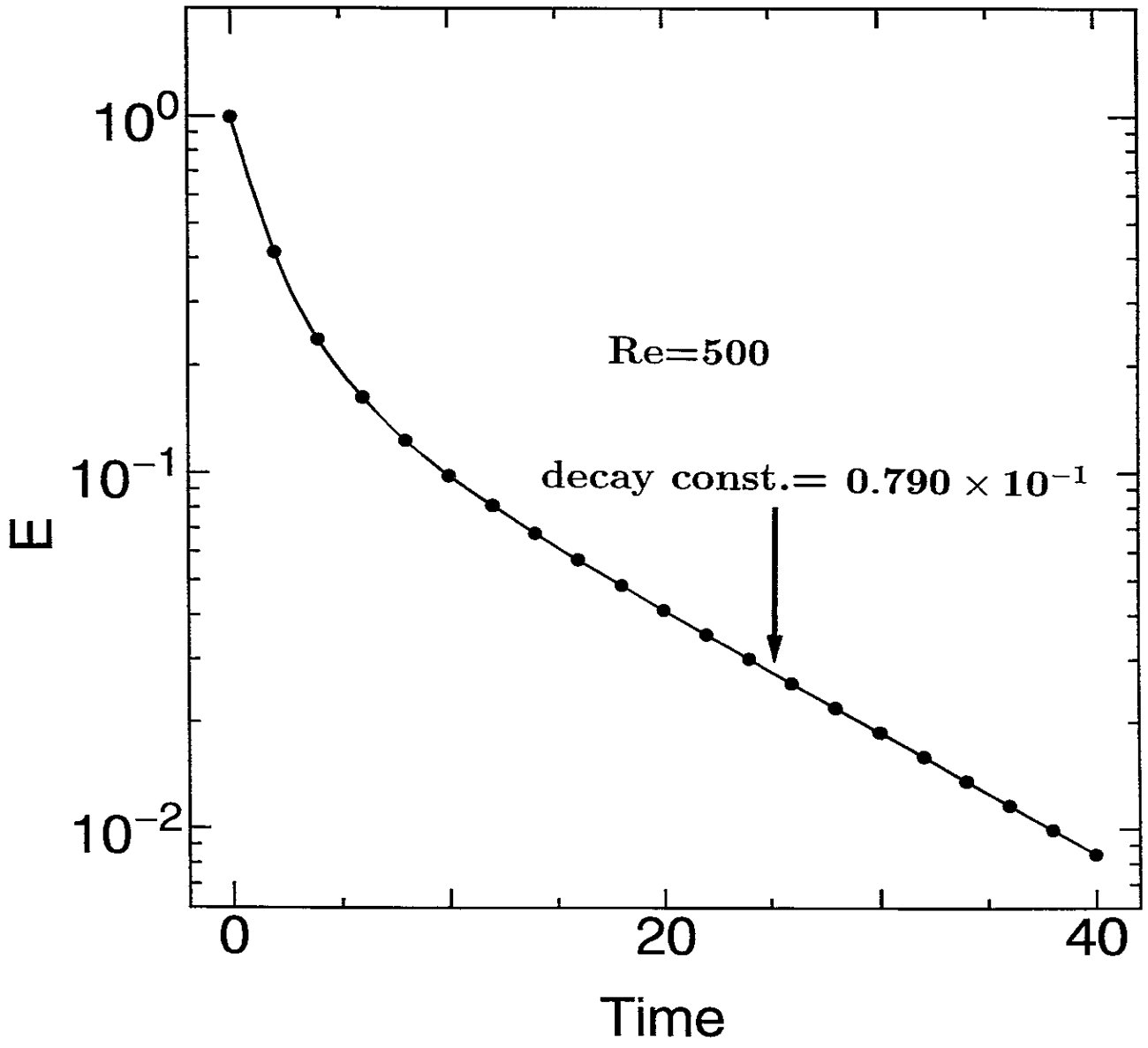

Fig.3

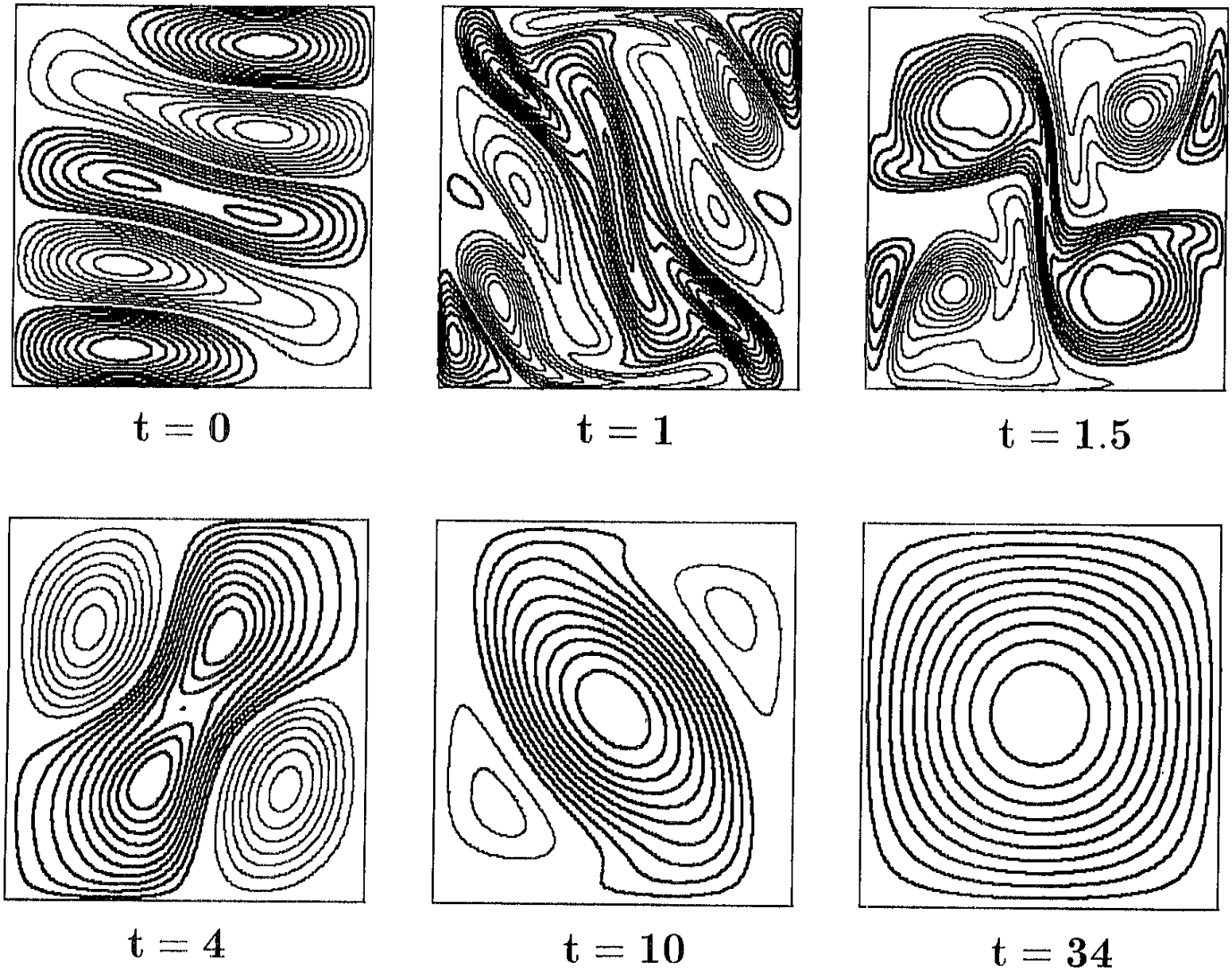

Fig. 4

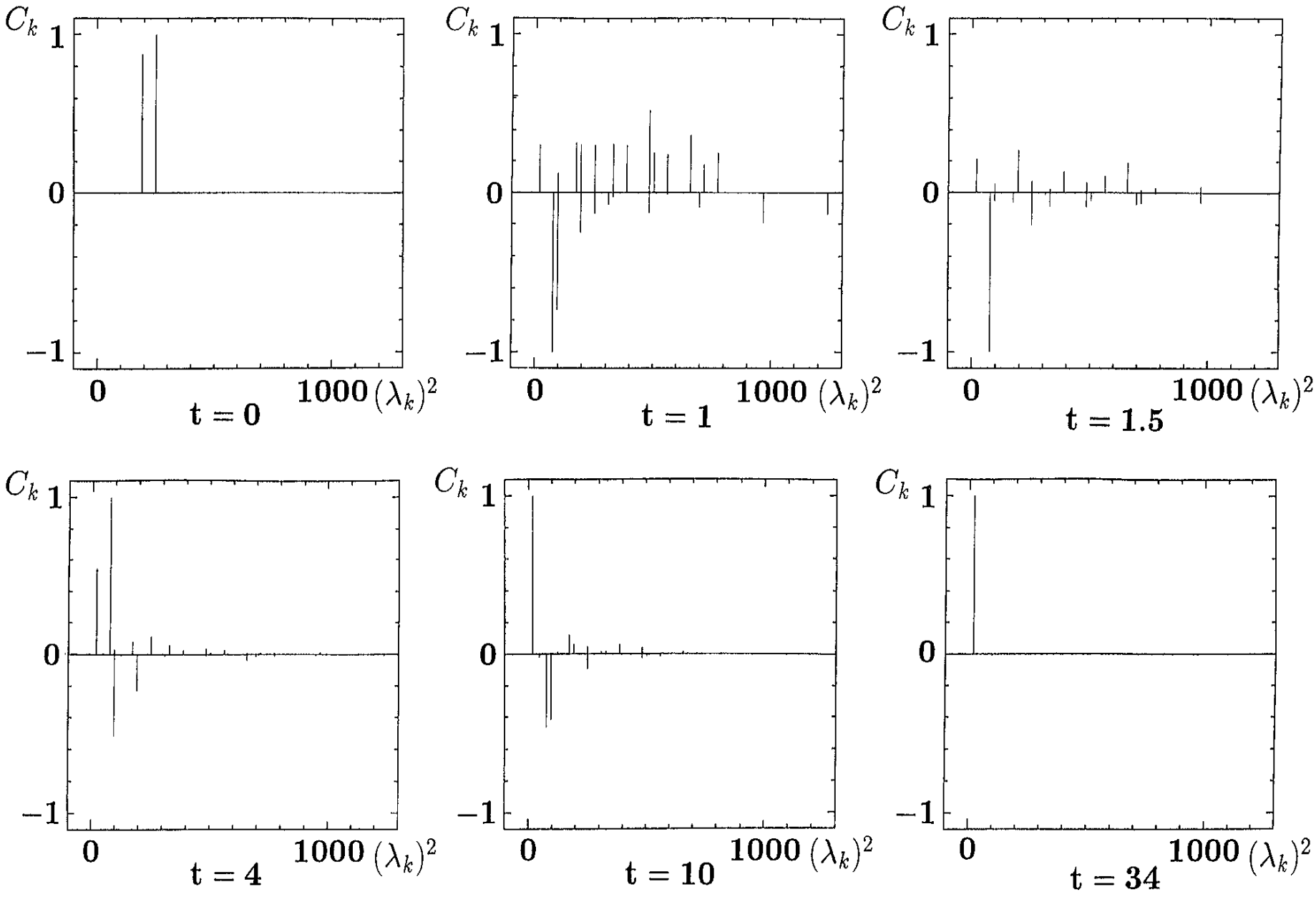

Fig. 5

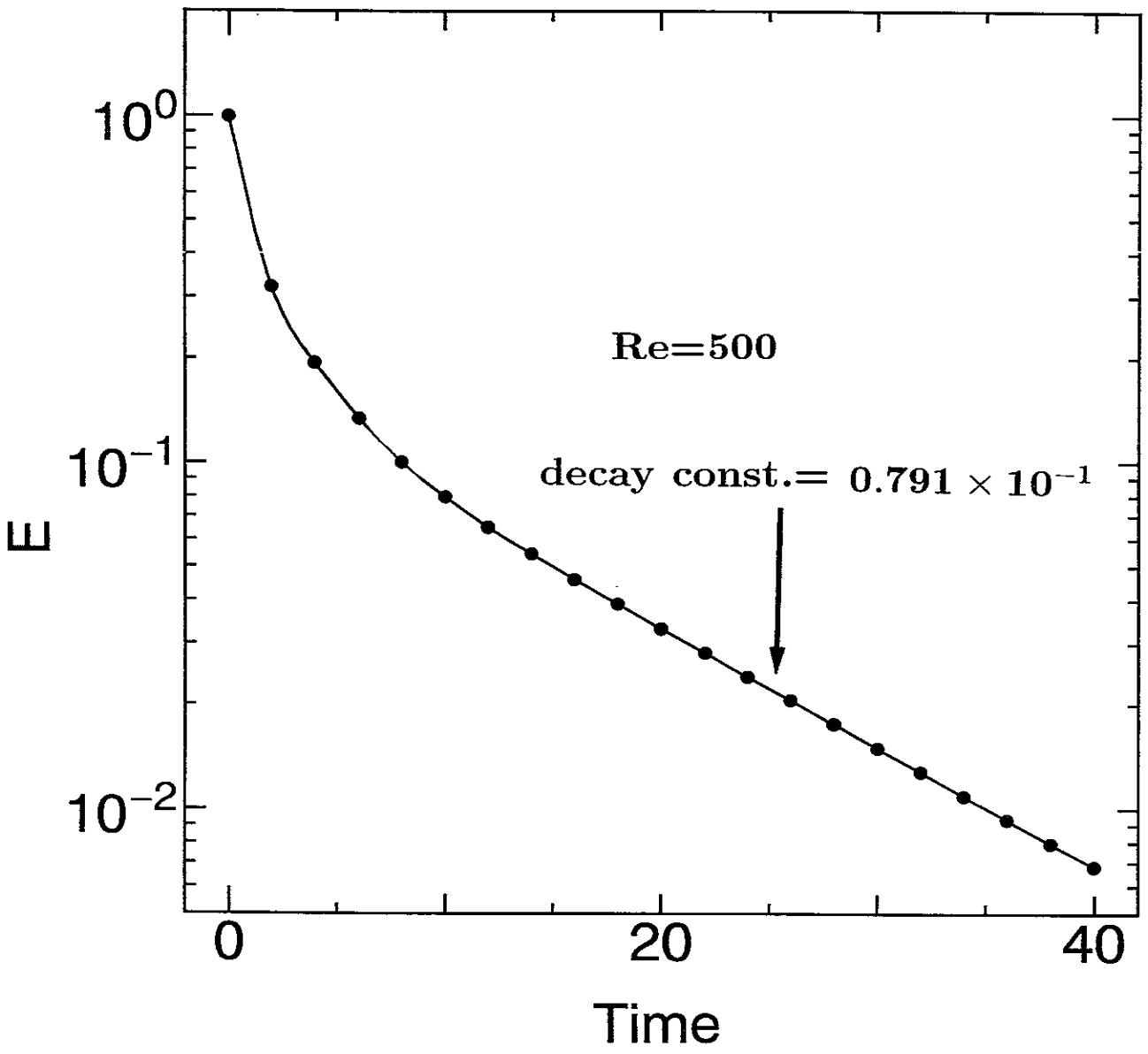

Fig. 6

Recent Issues of NIFS Series

NIFS-333 K. Itoh, S.-I. Itoh, M. Yagi, A. Fukuyama,
Theory of Anomalous Transport in Reverse Field Pinch; Jan. 1995

NIFS-334 K. Nagasaki, A. Isayama and A. Ejiri
Application of Grating Polarizer to 106.4GHz ECH System on Heliotron-E; Jan. 1995

NIFS-335 H. Takamaru, T. Sato, R. Horiuchi, K. Watanabe and Complexity Simulation Group,
A Self-Consistent Open Boundary Model for Particle Simulation in Plasmas; Feb. 1995

NIFS-336 B.B. Kadomtsev,
Quantum Telegragh : is it possible?; Feb. 1995

NIFS-337 B.B.Kadomtsev,
Ball Lightning as Self-Organization Phenomenon; Feb. 1995

NIFS-338 Y. Takeiri, A. Ando, O. Kaneko, Y. Oka, K. Tsumori, R. Akiyama, E. Asano, T. Kawamoto, M. Tanaka and T. Kuroda,
High-Energy Acceleration of an Intense Negative Ion Beam; Feb. 1995

NIFS-339 K. Toi, T. Morisaki, S. Sakakibara, S. Ohdachi, T.Minami, S. Morita, H. Yamada, K. Tanaka, K. Ida, S. Okamura, A. Ejiri, H. Iguchi, K. Nishimura, K. Matsuoka, A. Ando, J. Xu, I. Yamada, K. Narihara, R. Akiyama, H. Idei, S. Kubo, T. Ozaki, C. Takahashi, K. Tsumori,
H-Mode Study in CHS; Feb. 1995

NIFS-340 T. Okada and H. Tazawa,
Filamentation Instability in a Light Ion Beam-plasma System with External Magnetic Field; Feb. 1995

NIFS-341 T. Watanbe, G. Gnudi,
A New Algorithm for Differential-Algebraic Equations Based on HIDM; Feb. 13, 1995

NIFS-342 Y. Nejoh,
New Stationary Solutions of the Nonlinear Drift Wave Equation; Feb. 1995

NIFS-343 A. Ejiri, S. Sakakibara and K. Kawahata,
Signal Based Mixing Analysis for the Magnetohydrodynamic Mode Reconstruction from Homodyne Microwave Reflectometry; Mar.. 1995

NIFS-344 B.B.Kadomtsev, K. Itoh, S.-I. Itoh
Fast Change in Core Transport after L-H Transition; Mar. 1995

NIFS-345 W.X. Wang, M. Okamoto, N. Nakajima and S. Murakami,
An Accurate Nonlinear Monte Carlo Collision Operator; Mar. 1995

NIFS-346 S. Sasaki, S. Takamura, S. Masuzaki, S. Watanabe, T. Kato, K. Kadota,
Helium I Line Intensity Ratios in a Plasma for the Diagnostics of Fusion Edge Plasmas; Mar. 1995

NIFS-347 M. Osakabe,
Measurement of Neutron Energy on D-T Fusion Plasma Experiments; Apr. 1995

NIFS-348 M. Sita Janaki, M.R. Gupta and Brahmananda Dasgupta,
Adiabatic Electron Acceleration in a Cnoidal Wave; Apr. 1995

NIFS-349 J. Xu, K. Ida and J. Fujita,
A Note for Pitch Angle Measurement of Magnetic Field in a Toroidal Plasma Using Motional Stark Effect; Apr. 1995

NIFS-350 J. Uramoto,
Characteristics for Metal Plate Penetration of a Low Energy Negative Muonlike or Pionlike Particle Beam: Apr. 1995

NIFS-351 J. Uramoto,
An Estimation of Life Time for A Low Energy Negative Pionlike Particle Beam: Apr. 1995

NIFS-352 A. Taniike,
Energy Loss Mechanism of a Gold Ion Beam on a Tandem Acceleration System: May 1995

NIFS-353 A. Nishizawa, Y. Hamada, Y. Kawasumi and H. Iguchi,
Increase of Lifetime of Thallium Zeolite Ion Source for Single-Ended Accelerator: May 1995

NIFS-354 S. Murakami, N. Nakajima, S. Okamura and M. Okamoto,
Orbital Aspects of Reachable β Value in NBI Heated Heliotron/Torsatrons; May 1995

NIFS-355 H. Sugama and W. Horton,
Neoclassical and Anomalous Transport in Axisymmetric Toroidal Plasmas with Electrostatic Turbulence; May 1995

NIFS-356 N. Ohyabu
A New Boundary Control Scheme for Simultaneous Achievement of H-mode and Radiative Cooling (SHC Boundary); May 1995

NIFS-357 Y. Hamada, K.N. Sato, H. Sakakita, A. Nishizawa, Y. Kawasumi, R. Liang, K. Kawahata, A. Ejiri, K. Toi, K. Narihara, K. Sato, T. Seki, H. Iguchi,

A. Fujisawa, K. Adachi, S. Hidekuma, S. Hirokura, K. Ida, M. Kojima, J. Koong, R. Kumazawa, H. Kuramoto, T. Minami,. M. Sasao, T. Tsuzuki, J.Xu, I. Yamada, and T. Watari,
Large Potential Change Induced by Pellet Injection in JIPP T-IIU Tokamak Plasmas; May 1995

NIFS-358 M. Ida and T. Yabe,
Implicit CIP (Cubic-Interpolated Propagation) Method in One Dimension; May 1995

NIFS-359 A. Kageyama, T. Sato and The Complexity Simulation Group,
Computer Has Solved A Historical Puzzle: Generation of Earth's Dipole Field; June 1995

NIFS-360 K. Itoh, S.-I. Itoh, M. Yagi and A. Fukuyama,
Dynamic Structure in Self-Sustained Turbulence; June 1995

NIFS-361 K. Kamada, H. Kinoshita and H. Takahashi,
Anomalous Heat Evolution of Deuteron Implanted Al on Electron Bombardment; June 1995

NIFS-362 V.D. Pustovitov,
Suppression of Pfirsch-schlüter Current by Vertical Magnetic Field in Stellarators; June 1995

NIFS-363 A. Ida, H. Sanuki and J. Todoroki
An Extended K-dV Equation for Nonlinear Magnetosonic Wave in a Multi-Ion Plasma; June 1995

NIFS-364 H. Sugama and W. Horton
Entropy Production and Onsager Symmetry in Neoclassical Transport Processes of Toroidal Plasmas; July 1995

NIFS-365 K. Itoh, S.-I. Itoh, A. Fukuyama and M. Yagi,
On the Minimum Circulating Power of Steady State Tokamaks; July 1995

NIFS-366 K. Itoh and Sanae-I. Itoh,
The Role of Electric Field in Confinement; July 1995

NIFS-367 F. Xiao and T. Yabe,
A Rational Function Based Scheme for Solving Advection Equation; July 1995

NIFS-368 Y. Takeiri, O. Kaneko, Y. Oka, K. Tsumori, E. Asano, R. Akiyama, T. Kawamoto and T. Kuroda,
Multi-Beamlet Focusing of Intense Negative Ion Beams by Aperture Displacement Technique; Aug. 1995

NIFS-369 A. Ando, Y. Takeiri, O. Kaneko, Y. Oka, K. Tsumori, E. Asano, T. Kawamoto, R. Akiyama and T. Kuroda,
Experiments of an Intense H- Ion Beam Acceleration; Aug. 1995

NIFS-370 M. Sasao, A. Taniike, I. Nomura, M. Wada, H. Yamaoka and M. Sato,
Development of Diagnostic Beams for Alpha Particle Measurement on ITER; Aug. 1995

NIFS-371 S. Yamaguchi, J. Yamamoto and O. Motojima;
A New Cable -in conduit Conductor Magnet with Insulated Strands; Sep. 1995

NIFS-372 H. Miura,
Enstrophy Generation in a Shock-Dominated Turbulence; Sep. 1995

NIFS-373 M. Natsir, A. Sagara, K. Tsuzuki, B. Tsuchiya, Y. Hasegawa, O. Motojima,
Control of Discharge Conditions to Reduce Hydrogen Content in Low Z Films Produced with DC Glow; Sep. 1995

NIFS-374 K. Tsuzuki, M. Natsir, N. Inoue, A. Sagara, N. Noda, O. Motojima, T. Mochizuki, I. Fujita, T. Hino and T. Yamashina,
Behavior of Hydrogen Atoms in Boron Films during H_2 and He Glow Discharge and Thermal Desorption; Sep. 1995

NIFS-375 U. Stroth, M. Murakami, R.A. Dory, H. Yamada, S. Okamura, F. Sano and T. Obiki,
Energy Confinement Scaling from the International Stellarator Database; Sep. 1995

NIFS-376 S. Bazdenkov, T. Sato, K. Watanabe and The Complexity Simulation Group,
Multi-Scale Semi-Ideal Magnetohydrodynamics of a Tokamak Plasma; Sep. 1995

NIFS-377 J. Uramoto,
Extraction of Negative Pionlike Particles from a H2 or D2 Gas Discharge Plasma in Magnetic Field; Sep. 1995

NIFS-378 K. Akaishi,
Theoretical Consideration for the Outgassing Characteristics of an Unbaked Vacuum System; Oct. 1995

NIFS-379 H. Shimazu, S. Machida and M. Tanaka,
Macro-Particle Simulation of Collisionless Parallel Shocks; Oct. 1995

NIFS-380 N. Kondo and Y. Kondoh,
Eigenfunction Spectrum Analysis for Self-organization in Dissipative Solitons; Oct. 1995